The Extragalactic Infrared Background and its Cosmological Implications
IAU Symposium, Vol. 204, 2001
Martin Harwit and Michael G. Hauser, eds.

Gravitational Lensing and Deep Infrared Surveys

Leo Metcalfe
ISO Data Centre, Astrophysics Division, Space Science Department of ESA, Villafranca del Castillo, P.O.Box 50727, 28080 Madrid, Spain.

B. McBreen
Physics Department, University College Dublin, Stillorgan Road, Dublin 4, Ireland.

J.-P. Kneib
Observatoire Midi-Pyrénées, Laboratoire d'Astrophysique, UMR 5572, 14 Avenue E. Belin, F-31400 Toulouse, France.

B. Altieri
XMM Operations Centre, Astrophysics Division, Space Science Dept. of ESA, Villafranca del Castillo, P.O.Box 50727, 28080 Madrid, Spain.

Abstract. ISO's infrared camera was used to make deep mid-infrared (MIR) images through three gravitationally lensing clusters of galaxies. Observations were made at 7 μm and 15 μm covering more than 50 square arcminutes, with the lensing increasing the sensitivity to background sources significantly.

A large number of MIR sources were detected behind the lenses and provide source counts, corrected for cluster contamination and lensing distortion effects, which exceed by a factor of 10 the expectation from local counts assuming a no-evolution model. The results are consistent with larger-area surveys and the detected population resolves a substantial fraction (of order 60%) of the background MIR radiation intensity into discrete sources.

We discuss the evidence, in large part derived from lensing cluster observations, for overlap of the ISO 15 μm faint galaxy population with the 850 μm submillimetre and the 0.5 to 7 keV X-ray populations. We find that the ISO data shows substantial overlap with both the submillimetre and the X-ray source populations, with roughly 25% of ISO sources being detected at submillimetre wavelengths and a significant number of Chandra X-ray sources being detected in the ISO data.

1. Introduction

Following the identification of the first cosmological gravitational lens by Young et al. (1980) the theoretical and observational exploitation of the lensing phenomenon developed rapidly. In 1987 luminous giant arcs were discovered in the

https://doi.org/10.1017/S0074180900226119 Published online by Cambridge University Press

fields of some galaxy clusters by Lynds & Petrosian (1986), and independently by Soucail et al. (1987), and these were soon recognised to be Einstein rings (Paczyński 1987).

Since then observations of cluster-lenses have been extended to wavelengths other than the visible (e.g., Smail et al. 1993 - for the NIR; Smail et al. 1997 & Blain et al. 1999 - for the submillimetre region; Bautz et al. 2000 - for the X-ray). At the same time models describing the lensing have been refined (Kneib et al. 1996; Bezecourt et al. 1999) to the point where source counts made through a cluster lens can be corrected to yield the counts and source fluxes which would be found in the absence of the lens.

In a deep-survey programme, initiated almost a decade ago as part of the "Central Programme" of the ISO mission, we have extended the exploitation of the gravitational lensing phenomenon to the mid-infrared (MIR) by using ISOCAM (Cesarsky et al. 1996) on the Infrared Space Observatory (ISO, Kessler et al. 1996), launched by ESA in 1995.

The programme achieved deep and ultra-deep imaging through a sample of gravitationally lensing clusters of galaxies, benefiting from the lensing to search for background objects to a depth not otherwise achievable (Metcalfe et al. 1999; Altieri et al. 1999; Barvainis et al. 1999). Lensing amplifies sources and, for a given apparent flux limit, suppresses confusion, due to the apparent surface area dilation. To the flux-limits of this sample, even rich foreground galaxy clusters are essentially transparent at 15 μm. We find, in common with other deep ISOCAM surveys (Elbaz et al. 1999; Cesarsky - this conference; Elbaz - this Assembly; Serjeant et al. 2000), that we have resolved into discrete sources a significant fraction of the diffuse infrared background seen at 15 μm.

These MIR–luminous galaxies have been interpreted (Aussel et al. 1999b; Elbaz et al. 1999; Serjeant et al. 2000; Cesarsky - this conference) as a population of dust-enshrouded star forming galaxies. They have a median redshift of about 0.7.

Similarly, in recent years, observations through massive cluster lenses with well constrained mass models have played an important role in extending sub-millimetre (submm) observations to the deepest levels (Blain et al. 1999; Ivison et al. 2000). Sufficient submm sources have been resolved to account for a diffuse 850 μm background comparable to that measured by COBE (Fixsen et al. 1998). Blain et al. (2000) interpret the submm sources to be a population of distant, dusty galaxies emitting in the submm waveband, missing from optical surveys, and tracing dust obscured star formation activity at high redshift ($z \lesssim 5$). The total energy emitted is five times greater than inferred from restframe UV observations. They discuss the difficulty of distinguishing between star formation and recycling of AGN emission, as mechanisms for powering the submm emission. This couples to a long-standing question concerning the origin of the diffuse hard-X-ray background. The spectrum of this background in the 1 to 7 keV range is too flat to be traced to any known population of extragalactic sources. It could be synthesised if a component is attributed to highly obscured type 2 AGN (Setti & Woltjer 1989).

Following the advent of the orbiting Chandra X-ray observatory, Mushotzky et al. (2000) reported the resolution, by Chandra, of at least 75% of the 2 to 10 keV X-ray background into discrete sources.

https://doi.org/10.1017/S0074180900226119 Published online by Cambridge University Press

The question arises as to what is the relationship between the MIR, submm and X-ray faint galaxy populations? Are the MIR and submm populations all driven by star formation, or is the absorption and re-emission of energy from AGNs in dusty galaxies contributing significantly to counts at these wavelengths?

1.1. Overlap of the Populations

Hard X-ray (BeppoSAX) observations demonstrate that combined X-ray and IR observations provide the most powerful tool to characterize the absorbed AGN population, because they more directly probe the nuclear engine and the reprocessing in the nuclear environment (e.g., Vignati et al. 1999; Matt et al. 2000). The first Chandra surveys have unveiled a population of "optically-silent" AGN, making probably a substantial fraction of the XRB (Fiore et al. 2000; Mushotzky et al. 2000). If these objects are highly absorbed AGN and/or dusty galaxies, most of their output power might emerge in the IR. First results from the SCUBA surveys suggest that a fraction up to 20% of the FIR/submillimeter background is indeed due to dust-enshrouded AGN (Almaini et al. 1999), but this fraction could be higher if - as BeppoSAX results suggest - a substantial amount of absorbed AGN are Compton-thick (Maiolino et al. 1998; see also Fabian 1999 for a theoretical view).

Severgnini et al. (2000) compared observations, made with Chandra and SCUBA, of a sample of 34 sources at limiting fluxes sufficient to resolve most of the diffuse background in the two wavebands concerned. They sought to determine whether the submm and X-ray backgrounds arise in related phenomena. Out of 24 SCUBA sources they found that 23 were undetected by Chandra and concluded that, if the submm sources contain AGNs, these AGNs could not be giving rise to the 2-10 keV background, and that the presence, among the SCUBA-detected sources, of AGNs dominated by direct X-ray emission, seems very unlikely.

Ivison et al. (1998) and Soucail et al. (1999) described the properties of two lensed sources in the field of Abell 370, powered at least partially by AGNs, and having ISO counterparts.

Recently, Fabian et al. (2000) observed two massive galaxy clusters (Abell 2390 and Abell 1835) and compared the X-ray and submm fluxes of six SCUBA sources and four Chandra sources. They found only one marginal case of overlap. Wilman, Fabian, & Gandhi (2000) returned to the A2390 Chandra data to compare it with the ISO results of Lémonon et al. (1998) and Altieri et al. (1999). They reported that the two brightest Chandra X-ray sources have ISOCAM counterparts. They concluded that these objects are obscured AGN with the absorbed energy re-emitted in the infrared. It is clearly important to compare the results of Chandra and XMM surveys on ISO fields to further clarify the relationship between the hard X-ray (2 to 10 keV) faint galaxy population and the ISO 15 μm population.

Bautz et al. (2000) reported Chandra X-ray observations through the lensing cluster Abell 370, with detection of hard X-ray counterparts for the two prominent SCUBA sources. They concluded that their results are consistent with 20% of submm sources exhibiting significant AGN emission.

With reference to our ISO data and to the literature, we examined the overlap between the ISO 15 μm galaxy population and the submm and X-ray

https://doi.org/10.1017/S0074180900226119 Published online by Cambridge University Press

populations, and outline the latest information available on this topic from gravitational lensing studies. Thanks to the courtesy of R. Ivison and collaborators (private communications) we are able to go somewhat beyond the already published results, and remark upon ISO sources for which submm counterparts are under study.

Finally, we determine the contribution of our ISO MIR source population to the diffuse MIR background, showing that a large fraction of the background is resolved into discrete sources.

2. The ISO ARCS Mid-infrared Lensing Survey

2.1. The Observations

The fields of the well-known gravitationally lensing galaxy clusters Abell 370, Abell 2218 and Abell 2390 were observed using ISOCAM's 6.7 μm (LW2) and 14.3 μm (LW3) filters. The fields were observed in raster mode. The parameters for the rasters and the details of the instrument configurations used are given in Table 1.

By employing the CAM 3″ per-pixel field-of-view (PFOV) and raster step sizes which were multiples of 1/3 of a pixel, over many raster steps, we achieved a final mosaic pixel size of 1 arcsecond. The diameter of the PSF central maximum is $0.84\times\lambda(\mu\mathrm{m})$ arcseconds, so the FWHM is about half that amount. The final 1″ pixel size improved resolution and allowed better cross-identification with observations at other wavelengths. This strategy differs from many other CAM deep surveys which used the 6 arcsecond per-pixel field-of-view.

The rasters achieve greatest depth around their centres because the dwell time per position on the sky is a maximum in the centre of each raster. For purposes of data analysis and interpretation we divided the rasters into sensitivity zones. Table 1 indicates the limiting sensitivities achieved in each raster before correcting for the effects of cluster lensing.

2.2. The Benefits of Observing Through a Gravitational Lens

Figure 1 illustrates the action of a lensing cluster. The left hand image in the Figure shows a regular rectangular grid laid down over the field of the lensing cluster Abell 2218. The right hand image shows how that region of sky is transformed by the lens onto a plane on the background sky at a redshift of about 1, typical for our sources. The expansion of apparent surface area is very significant near the centre of the lens, and commensurate flux amplification and reduction of source confusion follow. The gain in the inner regions exceeds 5 over a significant area, and factors of more than 1.5 to 2 apply over much of the field illustrated by the rectangular grid.

To properly appreciate the benefit of the lensing survey it is necessary to consider, not simply the area of sky accessed to a given depth, but to fold in the number density of sources as a function of flux, in order to highlight the significant population of fainter sources made accessible by the lensing.

Figure 2 makes use of the surface density of sources on the sky as a function of flux, reported later in this paper, to compare the sample of sources accessible

https://doi.org/10.1017/S0074180900226119 Published online by Cambridge University Press

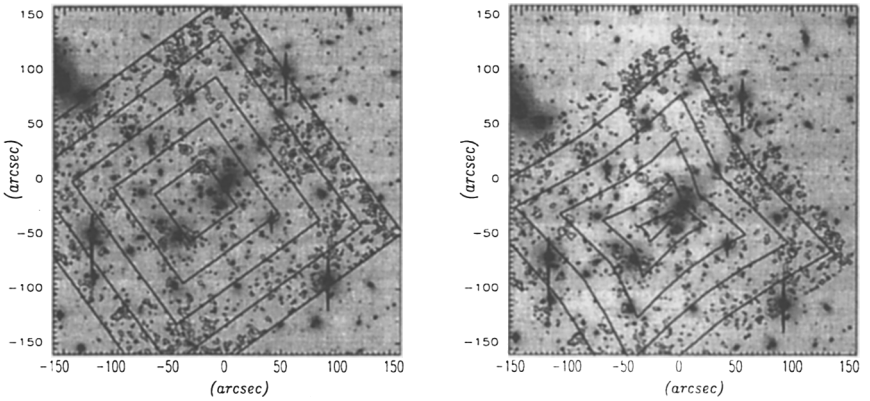

Figure 1. The grid shows how a region of sky as observed (image on the left) maps onto an actual area of sky behind the lens (image on the right). (Please see the discussion in the text.)

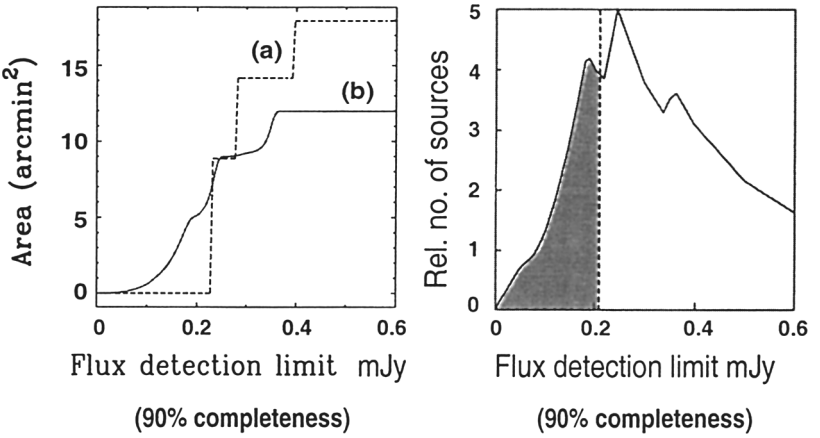

Figure 2. Increased sensitivity due to lensing: The plot on the left shows, for a typical case, how the area surveyed correlates with the limiting sensitivity : (a) without lensing - the dashed line; and (b) with lensing - the solid line. In the plot on the right the vertical line defines the sensitivity limit in the absence of lensing. The shaded region to the left of the line represents (quantitatively) the domain of additional sources that become accessible due to the presence of the lens.

https://doi.org/10.1017/S0074180900226119 Published online by Cambridge University Press

Table 1. Observational parameters and lensing clusters of galaxies used in the survey. On-chip integration time (t_{int}) was always 5.04 seconds and the 3″ per-pixel field-of-view was used. Sensitivity in μJy is quoted at the 80% completeness limit (cpl). Each raster was repeated m times.

Field	Filter†	Reads per step	n Steps M	N	dm asec	dn asec	area ($\prime^{-2}$)	μJy 80% cpl.	Done m times	Tot. t (sec.)
A2390	LW2	13	10	10	7	7	5.3	53	4	29300
	LW3	13	10	10	7	7	5.3	93	4	29300
A2218	LW2	14	12	12	16	16	16	75	2	22000
	LW3	14	12	12	16	16	16	207	2	22000
A370	LW2	10	14	14	22	22	31.3	80	2	22688
	LW3	10	14	14	22	22	31.3	293	2	22688

(†) LW2 and LW3 filters have reference wavelengths 6.7 and 14.3 μm, respectively.

in the absence of lensing with the sample which becomes accessible through making a lensing measurement.

In the graph on the left, the dashed line defines the area of sky accessible at a given limiting sensitivity in the absence of lensing. The curve is stepped because our measurements on the sky covered different regions to different depth. The solid line shows how the area of actual sky covered shrinks after lensing is taken into account. At the same time the limiting flux extends to fainter levels over some area of sky.

Lensing extends the accessible source population: In the plot on the right the measured number-density of sources on the sky, as a function of flux, has been folded with the area of sky covered to a given depth after lensing. It is seen that a significant population of sources below the unlensed sensitivity limit (shaded area) becomes accessible to the measurement.

Lensing also causes a surface dilation effect over the area probed. This spatial dilation is stronger towards the core of the cluster and increases with source-plane redshift. These effects need to be corrected during analysis in order to compare results with *blank* sky counts, such as those in the Hubble Deep field and Lockman Hole (Rowan-Robinson et al. 1997; Taniguchi et al. 1997; Aussel et al. 1999a; Elbaz et al. 1999).

The dilation of surface area acts to reduce source confusion. A lensing gain of n is associated with a surface area dilation by a factor n. For source counts having a slope with flux of -1.5 the area dilation just compensates for the increased depth achieved by the lensing, so that the apparent surface density of sources on the sky remains constant as one uses lensing to observe deeper. This means that source confusion, which would normally limit the depth to which observations can be made, is continually deferred. For populations yielding source counts around the critical slope of -1.5, an observation stopping just

https://doi.org/10.1017/S0074180900226119 Published online by Cambridge University Press

above the confusion limit on an unlensed field, may go much deeper on the lensed field, while still remaining unconfused.

3. ISO, SCUBA and Chandra - New Light on Distant Sources

In this section we describe some of the results of our ISO survey, and correlate them with some published results at submm (SCUBA) and X-ray (Chandra) wavelengths. In addition, Ivison and collaborators have kindly provided information concerning as yet unpublished submm detections, which allows more reliable inferences concerning the overlap between the MIR and submm populations.

The ISO 7 and 15 μm contour maps of Abell 2218 are overlaid on an optical image of the cluster in Figures 3 and 4, respectively. The differences between the two IR maps are striking. Many cluster sources and stars were detected in the 7 μm map - for example, in the vicinity of the two giant elliptical galaxies, whereas at 15 μm the cluster sources largely disappear, so that the bulk of the sources are background lensed objects. It should be noted that in the 15 μm map, the optical counterparts for even quite strong MIR sources are often quite faint.

In Figure 5, the contours of the ISO 15 μm map of Abell 370 are overlaid on an optical image of the cluster. The sources enclosed in dashed circles have been detected in the submm with SCUBA (Ivison et al. 1998; Smail et al. 1998) and were seen at hard X-ray energies with Chandra (Bautz et al. 2000). The object labeled (1) has the submm/X-ray identifier SMM 12399–0136(CX1) in the above references. The object labeled (2) has the identifier SMM 02399–0134(CX2) and has been discussed in some detail by Soucail et al. (1999). In the region of sky mapped by SCUBA, two out of seven ISO 15 μm sources have SCUBA counterparts.

In Figure 6, the contours of our ISO 15 μm map of Abell 2390 are overlaid on an optical image of the cluster. The peculiar core elliptical galaxy (Lémenon et al. 1999) was strongly detected. Other detections are mainly background lensed objects. The sources labeled A and B, which are, relative to this dataset, strong ISO 15 μm sources (0.38 ± 0.04 and 0.39 ± 0.04 mJy respectively — Metcalfe et al. 2001, in preparation) were detected with Chandra at hard X-ray energies — 1.5 to 7 keV (Fabian et al. 2000; Wilman et al. 2000). The ISO sources labeled C and D have coordinates within a few arcseconds (approximately 3) of the two further Chandra sources reported by Fabian et al. 2000 (this time only in the soft X-ray band, 0.5 to 2 keV). The ISO source positions, with accuracies of about ± 3 arseconds, are consistent with the nearby optical sources (one of which is the A2390 straight arc), and they are consistent with the published Chandra source coordinates. However, Fabian et al., with the higher astrometric accuracy achievable with Chandra, have rejected the optical sources close to the C and D ISO source positions as candidate counterparts for two nearby Chandra sources. The sources labeled 1 and 2 are SCUBA detections that have been reported in the literature (SMMJ 21535+1742 and SMMJ 21536+1742, respectively, in Smail et al. 1998). Submm (850μm) counterparts for the ISO sources labeled with numbers 3 to 5 are being studied by Ivison and collaborators (Ivison, private communication). Roughly 5 out of 23 ISO sources have candidate SCUBA

https://doi.org/10.1017/S0074180900226119 Published online by Cambridge University Press

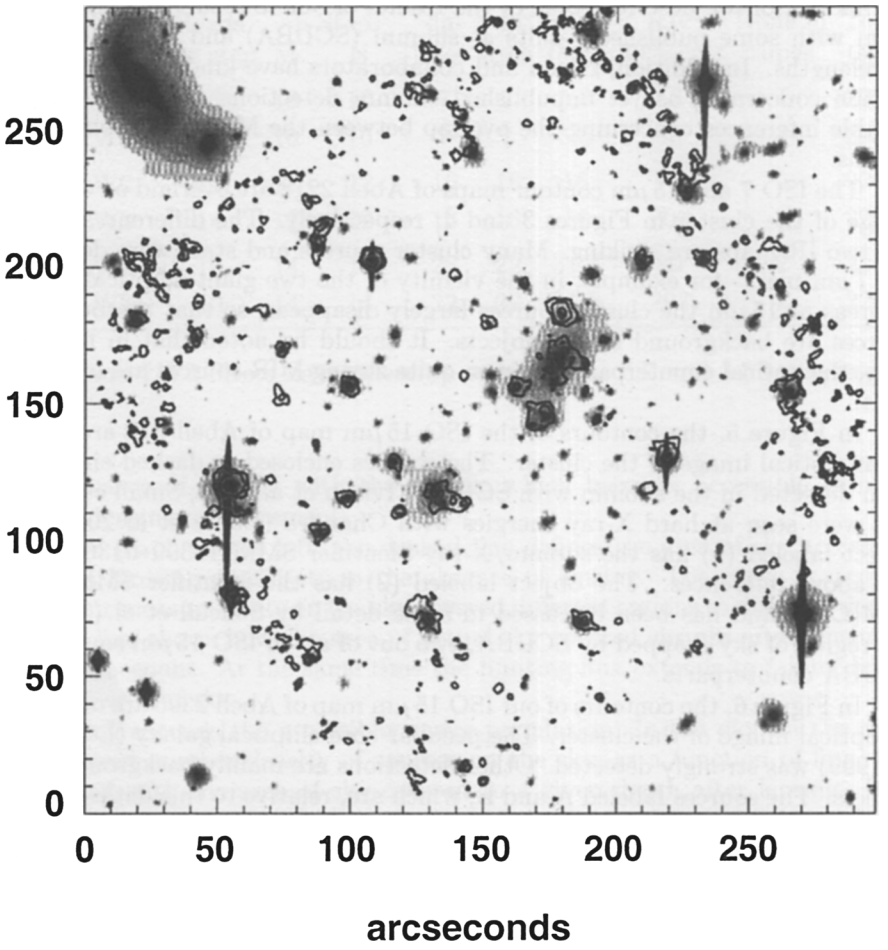

Figure 3. The ISOCAM 7 μm contour map of Abell 2218 overlaid on a deep Palomar 5-m I-band image (Smail, private communication). Many cluster sources and stars appear prominently in the map.

https://doi.org/10.1017/S0074180900226119 Published online by Cambridge University Press

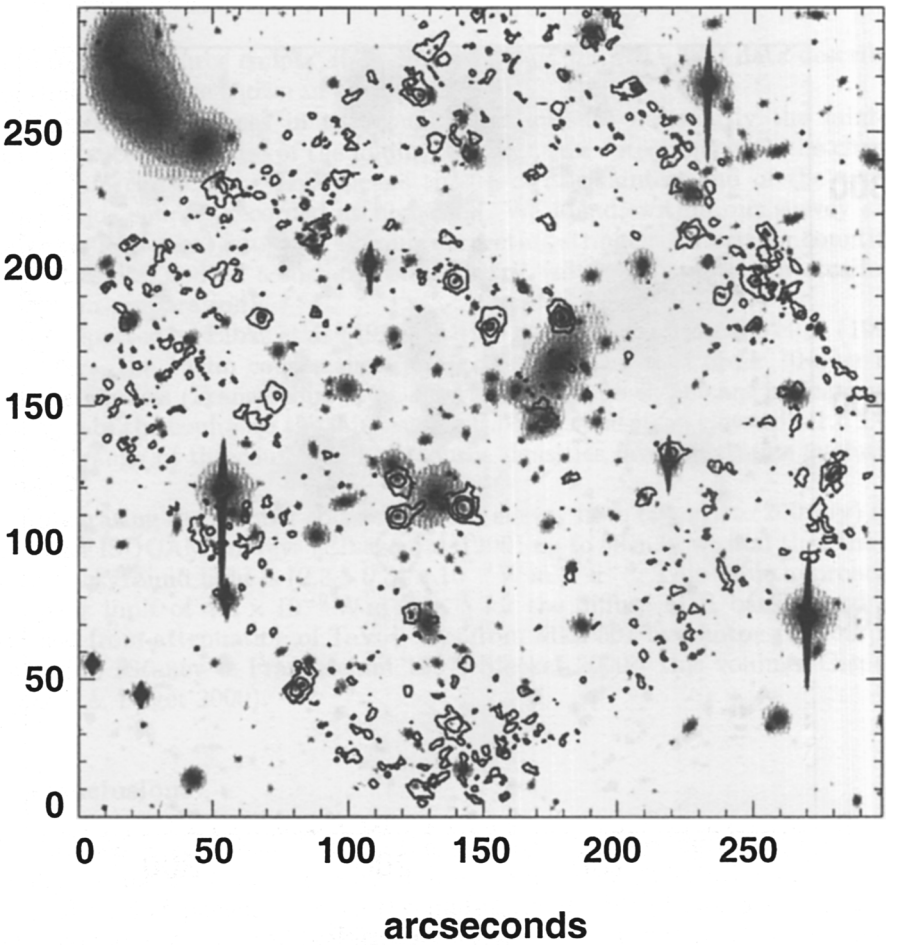

Figure 4. The ISOCAM 15 μm contour map of Abell 2218 overlaid on a deep Palomar 5-m I-band image. The IR sources are generally not from the same population as the known arclets. Cluster sources and stars are generally not detected.

https://doi.org/10.1017/S0074180900226119 Published online by Cambridge University Press

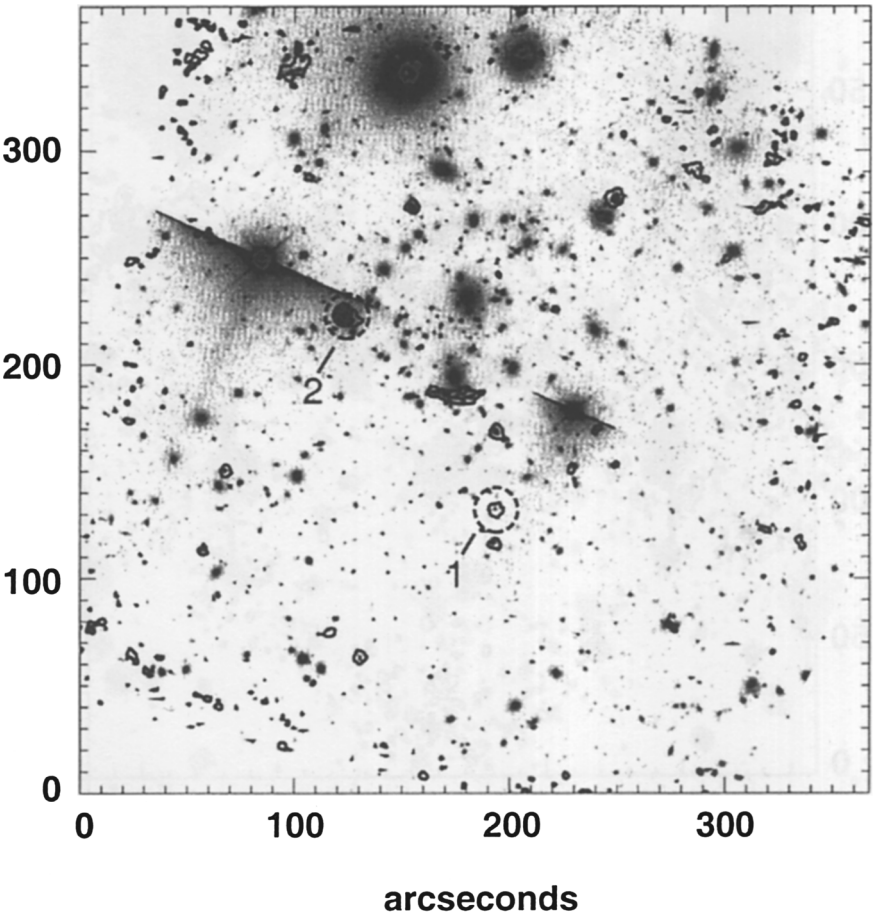

Figure 5. The ISOCAM 15 μm contour map of Abell 370 overlaid on a deep CFHT I-band image. The giant arc, near the centre of the map, was prominently detected. The two labeled sources have been detected at submm and X-ray wavelengths and are discussed in the text.

https://doi.org/10.1017/S0074180900226119 Published online by Cambridge University Press

counterparts. This is roughly the same proportion as seen in the A370 case – about 20 to 30%. At least two, and possibly all four, of the Chandra sources reported by Fabian et al. have ISO counterparts.

4. Source Counts at 15 μm

The integrated source counts at 15 μm, extracted from the ISO data described in outline above, are shown in Figure 7.

The faintest sources in the counts plot are not necessarily the faintest sources detected, because of the folding of the source detections with the cluster lensing gain correction. This means that even the faintest end of the source counts holds sources recorded at high S/N. We found, within our survey area (see Table 1 for area) a total of 42 sources meeting stringent criteria for counting. Refined results, and all associated photometry, will be reported by Metcalfe et al. 2001 (in preparation).

As reported by Elbaz et al. (1999), Altieri et al. (1999), Metcalfe et al. (1999) and others, the 15 μm counts show an excess by a factor of order 10 over no-evolution models (Franceschini et al. 1994). There is no significant indication of flattening of the counts to the faintest levels. The slope stays close to -1.6 ± 0.3 over the range of the counts. These source densities favour extreme evolution models.

Integrating the number counts over our survey from (50 μJy to 200 μJy) and over other ISOCAM surveys (Elbaz et al. 1999) up to 50 mJy we find that the resolved background light is $(2.3 \pm 0.8) \times 10^{-9}\,\mathrm{W\,m^{-2}\,sr^{-1}}$. This value approaches the upper limit of $4.0 \times 10^{-9}\,\mathrm{W\,m^{-2}\,sr^{-1}}$ for the diffuse MIR background determined from attenuation of TeV γ-rays from Mkn 501 by photon-photon pair production (Stanev & Franceschini 1997; Stecker 2000 - this volume; Gispert, Lagache, & Puget 2000).

5. Conclusions

We obtained a clear benefit from the strategy of observing through gravitationally lensing clusters of galaxies and extending the exploitation of the gravitational lensing phenomenon to the mid-infrared. We obtained much fainter source counts than we could otherwise have achieved. Lens models were reliable enough to permit us to correct for the effects of the lensing and obtain counts consistent, in the overlap region, with counts on unlensed fields.

Many 15 μm sources have very faint optical, and even K-band, counterparts. Our results are consistent with these sources being a population of dust-enshrouded star forming galaxies at moderate redshift (median redshift about 0.7).

About 20 to 30% of ISO 15 μm sources are detected at submm wavelengths. This overlap, coupled with the generally clear correlation between ISO sources and optical sources (albeit faint optical sources) could help to identify optical counterparts of SCUBA sources.

A significant number of hard X-ray sources are seen to emit at 15 μm, in contrast to the lack of any significant overlap between the submm and the X-ray

https://doi.org/10.1017/S0074180900226119 Published online by Cambridge University Press

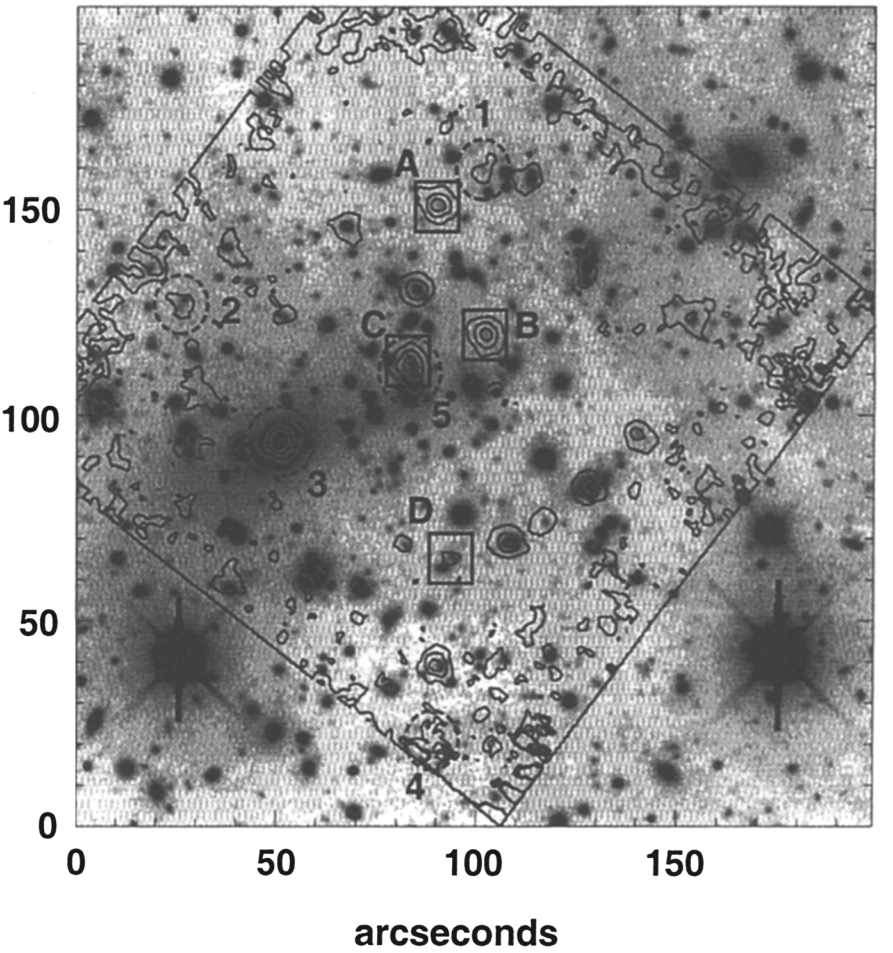

Figure 6. The ISOCAM 15 μm contour map of Abell 2390 overlaid on a deep I-band image. The sources inside squares and labeled A to D have ISO-derived positions consistent with the four Chandra detections reported by Fabian et al. (2000). Wilman et al. (2000) have discussed sources A and B. Sources 1 and 2, inside the dashed circles, have submm counterparts described in Smail et al. (1998). Submm counterparts of the ISO sources labeled 3 to 5 are being studied by Ivison and collaborators.

https://doi.org/10.1017/S0074180900226119 Published online by Cambridge University Press

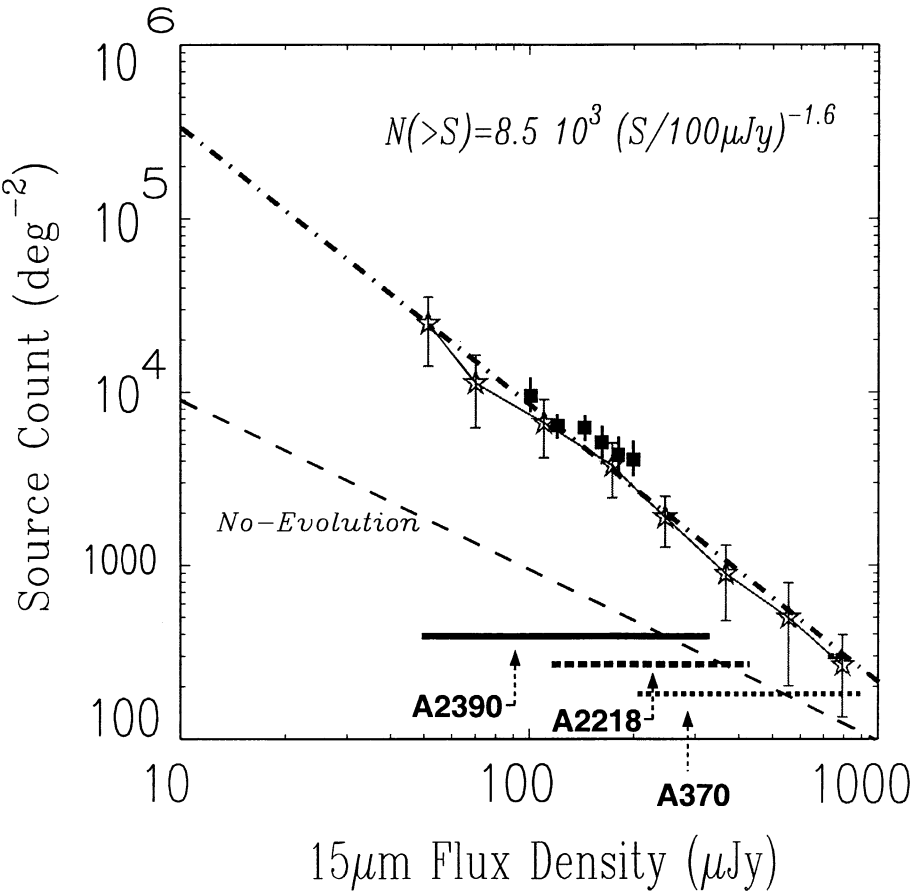

Figure 7. Lensing-corrected 15 μm source counts accumulated from the observations of the three lensing clusters. The black squares are the HDFN counts of Elbaz et al. (1999) & Aussel et al. (1999a). The three horizontal lines indicate the flux range addressed by each of the three clusters, after correction for lensing gain. The arrowed positions on the horizontal lines show where the counts would have stopped for that field in the absence of lensing. All counts below the arrow for each line are a direct benefit of observing through the gravitational lens.

https://doi.org/10.1017/S0074180900226119 Published online by Cambridge University Press

populations (Severgnini et al. 2000). The ISO population bridges the submm and X-ray populations.

We resolve a significant fraction (more than half) of the diffuse IR background at 15 μm into point sources.

Follow-up work is underway to make more quantitaive assessments of the overlaps of the submm and X-ray populations with the MIR population.

References

Almaini, O., Lawrence, A., & Boyle, B. J. 1999, MNRAS, 305, L59

Altieri, B., Metcalfe, L., Kneib, J-P. et al. 1999, A&A, 343, 65

Aussel, H., Cesarsky, C.J., Elbaz, D., & Starck, J.-L. 1999a, A&A, 342, 313

Aussel, H., Vigroux, L., Franceschini, A. et al. 1999b, American Astronomical Society Meeting 195, #09.17.

Barvainis., R., Antonucci R., & Helou., G. 1999, ApJ, 118, 645

Bautz, M. W., Malm, M. R., Baganoff, F. K., et al. 2000, ApJ, in press.

Bezecourt., J., Kneib, J.-P., Soucail, G., & Ebbels, T. 1999, A&A, 347, 21

Blain, A. W., Kneib, J.-P., Ivison, R. J., & Smail, I. 1999, ApJ, 512, L87

Blain, A. W., Smail, I., Ivison, R. J., & Kneib J.-P. 2000, MNRAS, 302, 632

Cesarsky, C. J., Abergel, A., Agnese, P., et al. 1996, A&A, 315, L32

Elbaz, D., Cesarsky, C. J., Fadda, D., et al. 1999, A&A, 351, L37

Fiore, F., La Franca, F., Vignali, C., et al. 2000, New Astronomy, 5, 143

Fabian, A. C. 1999, MNRAS, 308, L39

Fabian, A. C., Smail, I., Iwasawa, K., et al. 2000, MNRAS, 315, L8

Fixsen, D. J., Dwek, E., Mather, J. C., Bennett, C. L., & Shafer, R. A. 1998, ApJ, 508, 123

Franceschini, A., Mazzei, P., De Zotti, G., & Danese, L. 1994, ApJ, 427, 140

Gispert, R., Lagache, G., & Puget, J.-L. 2000, A&A, 360, 1

Ivison, R. J., Smail, I., Le Borgne, J.-F., et al. 1998, MNRAS, 298, 583

Ivison, R. J., Smail, I., Barger, A. J., et al. 2000, MNRAS, 315, 209

Kessler, M. F., Steinz, J. A., Anderegg, M., et al. 1996, A&A, 315, L27

Kneib, J-P., Ellis, R. S., Smail, I., Couch, W. J., & Sharples, R. M. 1996, ApJ, 471, 643

Lémonon, L., Pierre, M., Cesarsky, C. J., et al. 1998, A&A, 334, L21

Lynds, R., & Petrosian, V. 1986, BAAS, 18, 1014

Maiolino, R., Salvati, M., Bassani, L., et al. 1998, A&A, 338, 781

Matt, G., Pompilio, F., & La Franca, F. 2000, in Proceedings of the 20-22 September 1999 Workshop, Santorini, Greece, Large Scale Structure in the X-ray Universe, ed. M. Plionis & I. Georgantopoulos (Paris: Atlantisciences), 265

Metcalfe, L., Altieri, B., McBreen, B., et al. 1999, in The Universe as Seen by ISO, ed. P. Cox & M. F. Kessler, ESA-SP 427

Metcalfe, L., et al. 2001, in preparation

https://doi.org/10.1017/S0074180900226119 Published online by Cambridge University Press

Mushotzky, R. F., Cowie, L. L., Barger, A. J., & Arnaud, K. A. 2000, Nature, 404, 459

Paczyński, B. 1987, Nature, 325, 572

Pelló, R., LeBorgne, J. F., Soucail, G., Mellier, Y., & Sanahuja, B. 1991, ApJ, 366, 405

Rowan-Robinson, M., Mann, R., Oliver, S., et al. 1997, MNRAS, 289, 490

Serjeant, S., Oliver, S., Rowan-Robinson, M., et al. 2000, MNRAS, 316, 768

Setti, G., & Woltjer, L. 1989, A&A, 224, L21

Severgnini, P., Maiolino, R., Salvati, M., et al. 2000, A&A, 360, 457

Smail, I., Ellis, R., Aragoń-Salamanca, A., et al. 1993, MNRAS, 263, 628

Smail, I., Ivison, R. J., Blain, A. W., & Kneib, J.-P. 1998, ApJ, 507, L21

Smail, I., Ivison, R. J., & Blain, A. W. 1997, ApJ, 490, L5

Soucail, G., Mellier, Y., Fort, B., Mathez, G., & Cailloux, M. 1987, The Messenger, 50, 5

Soucail, G., Kneib, J.-P., Bzecourt, J., et al. 1999, A&A, 343, L70

Stanev, T., & Franceschini, A. 1997, ApJ, 494, L159

Taniguchi, Y., Cowie, L., Sato, Y., et al. 1997, A&A, 328, L9

Vignati, P., Molendi, S., Matt, G., et al. 1999, A&A, 349, L57

Wilman, R. J., Fabian, A. C., & Gandhi, P. 2000, MNRAS, 318, L11

Young, P., Gunn, J. E., Oke, J. B., Westphal, J., & Kristian, J. 1980, ApJ, 241, 507

Discussion

Catherine Cesarsky: What is the red shift domain of the sources seen by SCUBA and ISOCAM?

Leo Metcalfe: I mentioned in my presentation of SCUBA sources that the two ISOCAM counterparts in A370 have redshifts 2.8 and 1.06. In addition, three of the seven counterparts in A2390 have respective redshifts 1.52, 0.913, and 0.648. One target is the cluster dominant elliptical. Three sources have as yet no redshift assigned. The redshift of 1.52 is a photometric redshift.

David Jauncey: This is a beautiful use of gravitational lensing. However, rather than using or presenting integral source counts, it is preferable to use differential counts. This way there is a better indication of possible systematic and counting effects that may be present in your data, especially with such small numbers.

Metcalfe: Thank you for that comment! I had intended to show, during my presentation, the viewgraph of differential counts of all CAM mid-infrared surveys, which Catherine Cesarsky showed during her talk yesterday. But it slipped my mind. In any case, I fully agree. We should present our results also in the form of differential counts.

Metcalfe: Someone also raised the question whether the lensing correction could be refined by acquiring a better knowledge of the cluster mass distribution through comparing our observations on the clusters with observations off the cluster. The answer is that the cluster mass distribution in these cases was quite

https://doi.org/10.1017/S0074180900226119 Published online by Cambridge University Press

well determined. ROSAT X-ray observations traced well the mass distributions of the clusters. Also, in those cases where lensing arclets are seen for sources having known spectroscopic redshifts, the precise shape of the arclets can be used to constrain the lensing mass distribution. This is especially true when multiple images of the sources are seen. These clusters have been very well studied by such methods, especially at optical wavelengths, where one has the benefit of better spatial resolution.

https://doi.org/10.1017/S0074180900226119 Published online by Cambridge University Press